Published in final edited form as:
Clin Gastroenterol Hepatol. 2004 September ; 2(9): 744–753.

Optical Biopsy: A New Frontier in Endoscopic Detection and Diagnosis

THOMAS D. WANG and **JACQUES VAN DAM**
Division of Gastroenterology and Hepatology, Stanford University Medical Center, Stanford, California

Abstract

Endoscopic diagnosis currently relies on the ability of the operator to visualize abnormal patterns in the image created by light reflected from the mucosal surface of the gastrointestinal tract. Advances in fiber optics, light sources, detectors, and molecular biology have led to the development of several novel methods for tissue evaluation in situ. The term “optical biopsy” refers to methods that use the properties of light to enable the operator to make an instant diagnosis at endoscopy, previously possible only by using histological or cytological analysis. Promising imaging techniques include fluorescence endoscopy, optical coherence tomography, confocal microendoscopy, and molecular imaging. Point detection schemes under development include light scattering and Raman spectroscopy. Such advanced diagnostic methods go beyond standard endoscopic techniques by offering improved image resolution, contrast, and tissue penetration and providing biochemical and molecular information about mucosal disease. This review describes the basic biophysics of light-tissue interactions, assesses the strengths and weaknesses of each method, and examines clinical and preclinical evidence for each approach.

White light endoscopy currently is the primary method used for wide-area imaging in the gastrointestinal tract.[1] Because this method of detection is limited to the observation of reflected visible light from the mucosal surface, conventional endoscopy represents only the first of many possible methods to analyze tissue in vivo. The current practice of endoscopy often requires biopsies with ex vivo histological analysis and interpretation to make clinical decisions. This method of evaluation creates a significant delay in diagnosis, introduces the possibility of sampling error, and adds to the risk and cost of the procedure.[2–5] Furthermore, the lack of quantitative parameters for evaluation often results in significant interobserver and intraobserver variability.[6] Recent technological advances in fiber optics, light sources, detectors, and molecular biology have stimulated the unprecedented development of numerous optical methods that promise to significantly improve our ability to visualize and evaluate human epithelium in vivo.[7–12] These methods, collectively termed “optical biopsy,” are nondestructive in situ assays of mucosal histopathologic states using light that can provide instantaneous tissue assessment. In this review, the basic biophysics of light-tissue interaction and relevant clinical and preclinical data for each experimental method are presented.

Clinical end points for optical biopsy in the gastrointestinal tract are listed in Table 1. Primary goals include: (1) targeting premalignant mucosa for removal by biopsy, (2) grading and staging cancer progression, and (3) reducing the risk of physical biopsy. Cancer surveillance is challenging because the surface areas of disease involvement, such as that for Barrett’s esophagus and ulcerative colitis, are large, ranging from 10’s to 100’s of square centimeters.

Address requests for reprints to: Jacques Van Dam, M.D., Ph.D., Division of Gastroenterology and Hepatology, Stanford University Medical Center, 300 Pasteur Drive, Room H-1138, MC 5202, Stanford, California 94305. Fax: (650) 724-7495.
Dr. Wang has financial interest in the form of stock options in Optical Biopsies Technologies, Inc.

In addition, deep-tissue penetration of light is needed to detect lesions present below the mucosal surface, for example, the presence of abnormal glands beneath the squamous epithelium of the esophagus (Figure 1),[13,14] and to evaluate submucosal tumor invasion, in many instances to determine the appropriateness of endoscopic mucosal resection.[15,16] Thus, methods of imaging in the vertical cross-section (plane perpendicular to the mucosal surface) are needed. Furthermore, a comprehensive evaluation of disease may require visualization of subcellular features, such as nuclei (size, number, and chromatin content) and organelles.

All methods of optical imaging collect backscattered photons from the mucosa.[17–19] Conventional endoscopy observes reflected visible light (400–700 nm) from the mucosal surface. However, the light spectrum extends to shorter wavelengths in the ultraviolet (UV) and longer wavelengths in the near-infrared (NIR) that also can be used for endoscopic imaging (Figure 2). UV and blue light are absorbed by biomolecules to produce fluores-cence.[20] The visible band is dominated by hemoglobin absorption and thus has relatively short penetration depths, typically <100 μm, useful for imaging.[21] NIR light is much less sensitive to tissue scattering and hemoglobin absorption[20] and thus can usually penetrate <1000 μm through the mucosa.[22] Video endoscopes use charge-coupled device (CCD) detectors that are sensitive to both visible and NIR light.[23,24] Also, light can undergo elastic or inelastic scattering (Figure 3), in which the returning photons have the same or longer wavelength as that of the incident, respectively.[25] In addition, ballistic photons return through the tissue without additional scattering events and are useful for deep-tissue imaging, whereas diffuse photons return after several scattering events and are useful for measuring fine morphological structures.[26] In addition to imaging methods, point detection techniques can be used to collect molecular information during endoscopy with optical fiber probes inserted through the instrument channel. These methods have the potential to be extended to imaging. A description of the basic mechanism of how light interacts with tissue and the potential clinical use of each optical biopsy method discussed in this review is provided in Table 2.

Fluorescence Endoscopy

When biomolecules absorb light ($h\nu_a$), electrons elevate to greater energy levels, and subsequent relaxation to the energy ground state results in the emission of fluorescence ($h\nu_f$) at longer wavelengths (Figure 4).[21] Fluorescence can be collected from endogenous fluorophores, such as collagen, the reduced form of nicotinic-adenine dinucleotide, flavin adenine dinucleotide, and porphyrin.[27,28] Differences in peak wavelength and intensity between normal and diseased mucosa result from variations in the concentration and distribution of these metabolically active biomolecules and changes in tissue microarchitecture.[29–33]

The LIFE (light-induced fluorescence endoscope) system (Xillix Corp., Richmond, British Columbia, Canada) uses blue light (425–455 nm) from an xenon lamp for excitation, a fiber-optic endoscope to transmit fluorescence, and intensified CCD cameras for detection (Figure 5).[34–36] Fluorescence is spectrally divided into 2 color regimes by a dichroic mirror and then filtered into the green (480–580 nm) and red (620–720 nm) regions. Intensified cameras are needed because of the relatively weak fluorescence intensity. The white light image can still be detected with a color CCD camera. A ratio of the red to green images is determined to compensate for variations in the distance and angles from various sites of the mucosa. An example of a ratio fluorescence image of Barrett's esophagus collected in vivo using LIFE is shown in Figure 6.[35] The region of red enhancement (arrowheads) is suspicious for disease and was found to contain high-grade dysplasia (HGD) on histological examination. Clinical evidence for the usefulness of endogenous fluorescence endoscopy as a guide for biopsy is beginning to emerge with mixed results. A recent study using targeted biopsy performed first under endogenous fluorescence imaging with the LIFE system in 34 patients with short-

segment Barrett's esophagus found a greater number of sites of HGD than under subsequent conventional endoscopy (9 vs. 1 sites; $P = 0.016$).[37] In another study, 35 patients with Barrett's esophagus were evaluated first by autofluorescence endoscopy and then by random 4-quadrant biopsy.[38] However, fluorescence imaging was found to have a collective sensitivity of 21% for the detection of neoplastic lesions, including 88, 19, and 12 specimens of low-grade dysplasia (LGD), HGD, and cancer, respectively.

Biomolecules that accumulate in neoplastic cells and increase detection specificity and fluorescence intensity can be administered to patients harboring neoplasia. An example of such a biomolecule is aminolevulinic acid (ALA), a naturally occurring substrate in the heme synthetic pathway. ALA is converted intracellularly into protoporphyrin IX (PPIX).[39,40] The addition of exogenous ALA results in increased porphobilinogen deaminase levels and decreased ferrochelatase levels, which, in turn, cause greater production and retention of PPIX in neoplastic cells, respectively. Excitation is provided with blue light from a xenon lamp (375–440 nm bandpass filter). A longpass filter (450 nm) placed at the proximal end of a fiber-optic endoscope blocks reflected excitation light and allows the red PPIX fluorescence (>600 nm) for detection by a conventional (nonintensified) CCD camera.[41] An example of a fluorescence image collected ~6 hours after oral administration of ALA (15 mg/kg) shows increased red intensity at the site of the lesion (Figure 7), and well-differentiated carcinoma in situ was found on histological examination.[42] Clinical evidence of ALA use also was shown with quantitative measurements of exogenous PPIX fluorescence spectra from 20 patients with Barrett's esophagus administered oral ALA (10 mg/kg); it distinguished HGD from nondysplastic mucosa with a sensitivity and specificity of 77% and 71%, respectively.[43]

Optical Coherence Tomography

Optical coherence tomography (OCT) is novel method of imaging based on the principle of low-coherence interferometry.[44,45] A low-coherence source delivers modulated NIR light through an optical fiber that is then divided by a coupler (Figure 8). Most of the light is focused into the tissue by an objective, and the rest travels to a reference mirror.[46] Light returning from both paths is recombined by the coupler and detected. The signal is demodulated, digitized (A/D), and displayed. A light source with a short coherence length produces a signal only when the distance traveled by light in both paths of the interferometer are approximately the same. The intensity of the signal depends on the amount of light backscattered from tissue microstructures at a depth determined by the length of the reference path. The axial and transverse (lateral) resolutions are determined by the source coherence length and numerical aperture of the focusing objective, respectively, and typically are ~10 and 25 μm, respectively. Images are acquired at a rate of 4 frames/s, which is sufficient to avoid motion artifact.[47,48]

An OCT image collected in vivo from normal esophagus (Figure 9) obtained using a 2.4-mm diameter radial scan probe shows the discrete layers of mucosa, including squamous epithelium, lamina propria, muscularis mucosae, submucosa, lymph nodes, and muscularis externa.[46] Recently, high-resolution OCT prototypes showed an axial resolution ~2 μm.[49] Clinical studies have shown the ability of OCT to distinguish normal layers of esophageal mucosa and have defined image features of Barrett's esophagus, including: (1) the absence of normal layers populated by vertical pit and crypt morphological characteristics, (2) disorganized inhomogeneous architecture and an irregular mucosal surface, and (3) the presence of submucosal glands.[50,51] These criteria were evaluated prospectively and have a sensitivity and specificity of 97% and 92% for the detection of Barrett's, respectively. Furthermore, the ability to distinguish dysplasia in the colon in vivo was studied using colonic adenomas with 44 polyps in 24 patients (30 adenomas, 14 hyperplastic polyps). On OCT, adenomas, compared with hyperplastic polyps, had significantly less structure (organized crypt

pattern and mucosal layering) and light scattering (progression of intensity) by subjective appearance and less reflectance by digital image analysis.[52]

Confocal Microendoscopy

Confocal microscopy performs optical sectioning in tissue by eliminating photons that are out of focus.[53] Instruments designed for endoscopy use optical fibers with small-core diameters that function as a pinhole for collecting light that originates only from within a micron-sized volume of tissue.[54,55] Light scattered from outside the focus will not have the correct trajectory to enter the fiber. An image is created by 2-dimensional scanning, and a set of images collected over a range of depths can be used to generate a 3-dimensional image. The challenge of confocal microendoscopy is to achieve subcellular resolution and deep-tissue penetration with an instrument reduced to millimeter dimensions. The Optiscan confocal microscope (Optiscan Pty., Ltd., Notting Hill, Victoria, Australia) uses a single high numerical aperture lens. The scanning mechanism has dimensions of several millimeters and moves the fiber across the face of the objective.[56] This method collects fluorescence images with the use of intravenous fluorescein isothiocyanate–dextran for enhancing contrast.[57]

The dual-axes confocal architecture uses 2 low numerical aperture lenses to cross the illumination and collection beams at an angle (Figure 10) and has the ability to achieve 5-μm resolution at $\lambda = 1345$ nm in esophageal tissue ex vivo.[58] Furthermore, light scattered along the illumination path not in focus is not collected. In addition, this method is capable of collecting both reflectance and fluorescence[59] and thus can characterize cellular and tissue morphological characteristics, as well as detect biochemical and molecular changes in the mucosa. This architecture can be reduced to millimeter dimensions by using micro-electro-mechanical systems technology.[60] An ex vivo reflectance image was collected with a table-top prototype from a freshly excised biopsy specimen at the neosquamocolumnar junction (z-line) of a patient with Barrett's (Figure 11). The mucosa on the left half of the image appears to be organized into horizontal layers, which, by direct comparison to histological examination, correspond to epithelium, muscularis mucosa, submucosa, and muscularis propria.[58] The epithelium on the right half is disrupted by invaginating structures (arrows) that appear to be glands associated with the pit epithelium.

Light-Scattering Spectroscopy

Light-scattering spectroscopy (LSS) provides morphological information about such subcellular constituents as nuclei and mitochondria from elastically scattered visible light (Figure 4).[61] The spectrum from photons that undergo a single scattering event within the mucosa is obtained by first subtracting the contributions from multiple scattered light within the submucosa. A mathematical model is used to calculate the frequency and amplitude of oscillation of the collected spectrum to determine the size distribution and density of the scatterers, respectively.[62] Clinical evidence of this method for the detection of dysplasia has been shown in a study of 13 patients with 4, 5, 12, and 52 sites with HGD, LGD, indefinite for dysplasia, and nondysplastic intestinal metaplasia, respectively.[63] Logistic regression and cross-validation were used to compare the spectral classification with that of histopathologic examination. The sensitivity and specificity of LSS for detecting dysplasia (either LGD or HGD) were 90% and 90%, respectively, with all HGD and 87% of LGD sites correctly classified. This method has the potential to detect very early changes associated with cancer transformation.[64]

Raman Spectroscopy

Raman spectroscopy is performed by illuminating tissue with NIR photons that are absorbed by the unique vibrational/rotational modes of molecular bonds associated with chemical

functional groups specific to mucosal proteins, lipids, and nucleic acids (Figure 4).[65,66] A small fraction of these photons subsequently are inelastically scattered to form detailed spectral patterns that are often reduced to their principal components with multivariate statistics. However, the Raman effect is much weaker than that of fluorescence and can be obscured easily by fluorescence from the tissue or optical fiber itself. Recent advancement in CCD detector sensitivity and special filtered probes have allowed for the collection of Raman spectra in vivo.[67] Clinical evidence for the potential of this approach has been shown with the use of a laser diode at $\lambda = 785$ nm. Raman spectra were first collected ex vivo from 34 adenomatous and 20 hyperplastic polyps in 8 patients to validate the diagnostic algorithm and then collected in vivo from 10 adenomatous and 9 hyperplastic polyps in 3 patients to show the ability to distinguish polyp type with 100% sensitivity, 89% specificity, and 95% accuracy.[68]

Molecular Imaging

Molecular imaging is performed with the use of injected probes consisting of such small molecules as enzyme substrates, receptor ligands, monoclonal antibodies, and peptides tagged to a fluorescence dye to achieve high-affinity binding to specific biochemical and molecular markers of disease.[69] This approach is being developed primarily as a research tool with transgenic animals. The potential of this method has been shown with cathepsin B, a protease that has increased expression in neoplastic cells.[70] This probe is synthesized from a polymer tagged to Cy 5.5, an NIR dye, that is inactive in its native state, but releases fluorescence after being cleaved by cathepsin B. Figure 12 shows a fluorescence image of an excised specimen of the colon from an adenomatous polyposis coli (APC) min mouse after cathepsin B injection.[71] The image shows several large polyps ranging in diameter from 2–5 mm and several adenomas as small as 50 μm (arrows). Microendoscopes are being developed to study this method in vivo.[72]

Discussion

Performance parameters, including field of view, tissue penetration depth, spatial resolution, and image contrast, for the optical biopsy methods presented are listed in Table 3. A large field sufficient to perform wide-area surveillance can be achieved with fluorescence imaging by using conventional fiber-optic endoscopes. Tissue penetration through the mucosa is achieved with methods that use NIR light, including fluorescence and molecular imaging, OCT, and confocal microscopy, techniques that use visible light image no further than ~100 μm below the mucosal surface. Subcellular imaging requires high spatial resolution in both the axial and transverse dimension, which has been accomplished to date only with confocal microendoscopy. It is conceivable that ultrahigh-resolution OCT methods that use high bandwidth lasers may ultimately achieve this level of performance. Fiber-optic endoscopes do not perform optical sectioning and thus have poor axial resolution. Methods based on reflectance only, such as OCT, have image contrast limited to the intrinsic differences in tissue refractive index, whereas techniques that use fluorescence have the potential for significantly better contrast, depending on the mechanism used. A glossary of technical terms is presented in Table 4.

Ultimately, the clinical success of each method of optical biopsy will depend on the extent of additional improvements in detection sensitivity and specificity and on instrument cost. Also, accurate histological validation of these techniques must be performed and can be achieved using endoscopes equipped with dual-instrument channels for proper registration of the optical and standard pinch biopsies. Furthermore, large-scale clinical trials are needed to validate and standardize these technologies, building confidence in the medical community for their use. Fluorescence endoscopy offers the advantage of wide-area surveillance; however, artifacts may be introduced by the presence of such metabolic changes as inflammation, ischemia, and blood.

In addition, such structural changes as collagen thickening in polypoid lesions may crowd out sources of endogenous fluorescence. Low-noise CCD detectors with greater sensitivity are being developed for video collection of fluorescence. OCT offers wide-area vertical cross-sectional imaging with high resolution, but this method is not sensitive to fluorescence and the image resolution is degraded by a speckle pattern associated with coherent light. Confocal microendoscopy is sensitive to both reflectance and fluorescence with subcellular resolution. However, the field of view is limited, and, presently, this technique has been shown ex vivo only. Although point spectroscopy methods that use light scattering offer detailed information about tissue microstructure and molecular bonds, their use is likely to be primarily as an adjunct to imaging methods because of the small volume of tissue sampled. Raman spectroscopy faces the additional challenge of sufficient signal collection to perform real-time diagnostics.

At the present time, clinicians should resist the temptation to use these very promising, but experimental, technologies in making patient management decisions. Available data, although highly encouraging, are insufficient to allow us to draw conclusions about the optimal manner in which to screen and survey patients during endoscopy. The most successful clinical methods of optical biopsy likely will evolve in the form of a combination of imaging techniques that can provide wide-area surveillance, deep-tissue penetration, and high subcellular resolution, with possibly the addition of point detection methods for special applications. Future surveillance with endoscopy likely will include wide-area surveillance with fluorescence using NIR molecular probes that have high sensitivity and specificity to premalignant lesions present through the mucosa. The first disease targets likely will be flat dysplasia, such as that associated with Barrett's esophagus and ulcerative colitis. The cost and size of image detectors necessary for fluorescence detection have been decreasing steadily. As an adjunct, point detection methods and confocal microendoscopy can be used to further evaluate target lesions. These instruments can be reliably and inexpensively mass produced with use of optical fibers and micro-electro-mechanical systems technology.

The advances in endoscopic imaging described in this review provide a preview of the many exciting diagnostic possibilities that may soon enhance conventional endoscopy. Clinical and preclinical evidence suggest significant improvements can be achieved in terms of image resolution and tissue penetration, in addition to biochemical and molecular information about disease processes. Standard endoscopic imaging may be joined by fluorescence endoscopy for enhanced visualization of the mucosal surface. Greater disease specificity may be feasible with the administration of exogenous agents, such as high-affinity probes. Moreover, light emerging from deep within tissue can be imaged with high resolution by using molecular imaging, OCT, or confocal microendoscopy. Furthermore, detailed morphological and molecular information can be acquired with light-scattering and Raman spectroscopy, respectively. These methods of optical biopsy are unlikely to replace conventional biopsy with histopathologic interpretation of excised tissue at any time soon. Rather, they are more likely to provide a more accurate and efficient approach to target biopsy of diseased tissue, thus reducing the number of conventional biopsies required, increasing surveillance intervals, and reducing cost.

References

1. Sivak, MV. Gastroenterologic endoscopy. Philadelphia: Saunders; 1988.
2. Provenzale D, Onken J. Surveillance issues in inflammatory bowel disease: ulcerative colitis. J Clin Gastroenterol 2001;32:99–105. [PubMed: 11205664]
3. Reid BJ, Blount PL, Feng Z, Levine DS. Optimizing endoscopic biopsy detection of early cancers in Barrett's high-grade dysplasia. Am J Gastroenterol 2000;95:3089–3096. [PubMed: 11095322]
4. Levine DS, Haggitt RC, Blount PL, Rabinovitch PS, Rusch VW, Reid BJ. An endoscopic biopsy protocol can differentiate high-grade dysplasia from early adenocarcinoma in Barrett's esophagus. Gastroenterology 1993;105:40–50. [PubMed: 8514061]

5. Reid BJ, Weinstein WM, Lewin KJ, Haggitt RC, VanDeventer G, DenBesten L, Rubin CE. Endoscopic biopsy can detect high-grade dysplasia or early adenocarcinoma in Barrett's esophagus without grossly recognizable neoplastic lesions. Gastroenterology 1988;94:81–90. [PubMed: 3335302]
6. Riddell RH, Goldman H, Ransohoff DF, Appelman HD, Fenoglio CM, Haggitt RC, Ahren C, Correa P, Hamilton SR, Morson BC, et al. Dysplasia in inflammatory bowel disease: standardized classification with provisional clinical applications. Hum Pathol 1983;14:931–968. [PubMed: 6629368]
7. Van Dam J. Novel methods of enhanced endoscopic imaging. Gut 2003;52(suppl):S12–S16.
8. Ell C. Improving endoscopic resolution and sampling: fluorescence techniques. Gut 2003;52 (suppl):S30–S33.
9. Wang T, Triadafilopoulos GSMLXL. Gut 2003;52:5–7. [PubMed: 12477746]
10. Dacosta RS, Wilson BC, Marcon NE. New optical technologies for earlier endoscopic diagnosis of premalignant gastrointestinal lesions. J Gastroenterol Hepatol 2002;17(suppl):S85–S104. [PubMed: 12000596]
11. Pfau PR, Sivak MV Jr. Endoscopic diagnostics. Gastroenterology 2001;120:763–781. [PubMed: 11179249]
12. Drezek RA, Richards-Kortum R, Brewer MA, Feld MS, Pitris C, Ferenczy A, Faupel ML, Follen M. Optical imaging of the cervix. Cancer 2003;98:2015–2027. [PubMed: 14603538]
13. Biddlestone LR, Barham CP, Wilkinson SP, Barr H, Shepherd NA. The histopathology of treated Barrett's esophagus: squamous reepithelialization after acid suppression and laser and photodynamic therapy. Am J Surg Pathol 1998;22:239–245. [PubMed: 9500226]
14. Berenson MM, Johnson TD, Markowitz NR, Buchi KN, Samowitz WS. Restoration of squamous mucosa after ablation of Barrett's esophageal epithelium. Gastroenterology 1993;104:1686–1691. [PubMed: 8500727]
15. Ono H, Kondo H, Gotoda T, Shirao K, Yamaguchi H, Saito D, Hosokawa K, Shimoda T, Yoshida S. Endoscopic mucosal resection for treatment of early gastric cancer. Gut 2001;48:225–229. [PubMed: 11156645]
16. Noda M, Kodama T, Atsumi M, Nakajima M, Sawai N, Kashima K, Pignatelli M. Possibilities and limitations of endoscopic resection for early gastric cancer. Endoscopy 1997;29:361–365. [PubMed: 9270916]
17. Mourant JR, Hielscher AH, Eick AA, Johnson TM, Freyer JP. Evidence of intrinsic differences in the light scattering properties of tumorigenic and nontumorigenic cells. Cancer 1998;84:366–374. [PubMed: 9915139]
18. Hebden JC, Arridge SR, Delpy DT. Optical imaging in medicine: I. Experimental techniques Phys Med Biol 1997;42:825–840.
19. Cheong W, Prahl S, Welch AJ. A review of the optical properties of biological tissues. IEEE J Quant Electr 1990;26:2166–2185.
20. Bigio IJ, Mourant JR. Ultraviolet and visible spectroscopies for tissue diagnostics: fluorescence spectroscopy and elastic-scattering spectroscopy. Phys Med Biol 1997;42:803–814. [PubMed: 9172260]
21. Richards-Kortum R, Sevick-Muraca E. Quantitative optical spectroscopy for tissue diagnosis. Annu Rev Phys Chem 1996;47:555–606. [PubMed: 8930102]
22. Zonios G, Cothren R, Crawford JM, et al. Spectral pathology. Ann N Y Acad Sci 1998;838:108–115. [PubMed: 9511799]
23. Borotto E, Englender J, Pourny JC, Naveau S, Chaput JC, Lecarpentier Y. Detection of the fluorescence of GI vessels in rats using a CCD camera or a near-infrared video endoscope. Gastrointest Endosc 1999;50:684–688. [PubMed: 10536328]
24. Tsuji S, Kawano S, Sato N, Hayashi N, Peng HB, Tsujii M, Nagano K, Takei Y, Chen SS, Kashiwagi T, et al. Comparison of infrared electronic endoscopy using reflection and transmission. Endoscopy 1993;25:278–281. [PubMed: 8330546]
25. Fang H, Ollero M, Vitkin E, Kimerer LM, Cipolloni PB, Zaman MM, Freedman SD, Bigio IJ, Itzkan I, Hanlon EB, Perelman LT. Noninvasive sizing of subcellular organelles with light scattering spectroscopy. IEEE Journal of Selected Topics in Quantum Electronics 2003;9:267–276.

26. Mourant JR, Freyer JP, Hielscher AH, Eick AA, Shen D, Johnson TM. Mechanisms of light scattering from biological cells relevant to noninvasive optical-tissue diagnostics. Appl Optics 1998;37:3586–3593.
27. Zonios GI, Cothren RM, Arendt JT, Wu J, Van Dam J, Crawford JM, Manoharan R, Feld MS. Morphological model of human colon tissue fluorescence. IEEE Trans Biomed Eng 1996;43:113–122. [PubMed: 8682522]
28. Schomacker KT, Frisoli JK, Compton CC, Flotte TJ, Richter JM, Nishioka NS, Deutsch TF. Ultraviolet laser-induced fluorescence of colonic tissue: basic biology and diagnostic potential. Lasers Surg Med 1992;12:63–78. [PubMed: 1614265]
29. Bourg-Heckly G, Blais J, Padilla JJ, Bourdon O, Etienne J, Guillemin F, Lafay L. Endoscopic ultraviolet-induced autofluorescence spectroscopy of the esophagus: tissue characterization and potential for early cancer diagnosis. Endoscopy 2000;32:756–765. [PubMed: 11068834]
30. Panjehpour M, Overholt BF, Vo-Dinh T, Haggitt RC, Edwards DH, Buckley FP. Endoscopic fluorescence detection of high-grade dysplasia in Barrett's esophagus. Gastroenterology 1996;111:93–101. [PubMed: 8698231]
31. Izuishi K, Tajiri H, Fujii T, Boku N, Ohtsu A, Ohnishi T, Ryu M, Kinoshita T, Yoshida S. The histological basis of detection of adenoma and cancer in the colon by autofluorescence endoscopic imaging. Endoscopy 1999;31:511–516. [PubMed: 10533733]
32. Wang TD, Crawford JM, Feld MS, Wang Y, Itzkan I, Van Dam J. In vivo identification of colonic dysplasia using fluorescence endoscopic imaging. Gastrointest Endosc 1999;49:447–455. [PubMed: 10202057]
33. Wang TD, Van Dam J, Crawford JM, Preisinger EA, Wang Y, Feld MS. Fluorescence endoscopic imaging of human colonic adenomas. Gastroenterology 1996;111:1182–1191. [PubMed: 8898631]
34. Lam S, MacAulay C, Hung J, LeRiche J, Profio AE, Palcic B. Detection of dysplasia and carcinoma in situ using a lung imaging fluorescence endoscopy (LIFE) device. J Thorac Cardiovasc Surg 1993;105:1035–1040. [PubMed: 8501931]
35. Haringsma J, Tytgat GNJ, Yano H, Iishi H, Tatsuta M, Ogihara T, Watanabe H, Sato N, Marcon N, Wilson BC, Cline RW. Autofluorescence endoscopy: feasibility of detection of GI neoplasms unapparent to white light endoscopy with an evolving technology. Gastrointest Endosc 2001;53:642–650. [PubMed: 11323596]
36. Kobayashi M, Tajiri H, Seike E, Shitaya M, Tounou S, Mine M, Oba K. Detection of early gastric cancer by a real-time autofluorescence imaging system. Cancer Lett 2001;165:155–159. [PubMed: 11275364]
37. Niepsuj K, Niepsuj G, Cebula W, Zieleznik W, Adamek M, Sielanczyk A, Adamczyk J, Kurek J, Sieron A. Autofluorescence endoscopy for detection of high-grade dysplasia in short-segment Barrett's esophagus. Gastrointest Endosc 2003;58:715–719. [PubMed: 14595307]
38. Egger K, Werner M, Meining A, Ott R, Allescher HD, Hofler H, Classen M, Rosch T. Biopsy surveillance is still necessary in patients with Barrett's oesophagus despite new endoscopic imaging techniques. Gut 2003;52:18–23. [PubMed: 12477753]
39. Messmann H, Endlicher E, Freunek G, Rummele P, Scholmerich J, Knuchel R. Fluorescence endoscopy for the detection of low and high grade dysplasia in ulcerative colitis using systemic or local 5-aminolaevulinic acid sensitisation. Gut 2003;52:1003–1007. [PubMed: 12801958]
40. Messmann H, Knuchel R, Baumler W, Holstege A, Scholmerich J. Endoscopic fluorescence detection of dysplasia in patients with Barrett's esophagus, ulcerative colitis, or adenomatous polyps after 5-aminolevulinic acid-induced protoporphyrin IX sensitization. Gastrointest Endosc 1999;49:97–101. [PubMed: 9869731]
41. Mayinger B, Reh H, Hochberger J, Hahn EG. Endoscopic photo-dynamic diagnosis: oral aminolevulinic acid is a marker of GI cancer and dysplastic lesions. Gastrointest Endosc 1999;50:242–246. [PubMed: 10425420]
42. Mayinger B, Neidhardt S, Reh H, Martus P, Hahn EG. Fluorescence induced with 5-aminolevulinic acid for the endoscopic detection and follow-up of esophageal lesions. Gastrointest Endosc 2000;54:572–578. [PubMed: 11677472]
43. Brand S, Wang TD, Schomacker KT, Poneros JM, Lauwers GY, Compton CC, Pedrosa MC, Nishioka NS. Detection of high-grade dysplasia in Barrett's esophagus by spectroscopy measurement of 5-

aminolevulinic acid-induced protoporphyrin IX fluorescence. Gastrointest Endosc 2002;56:479–487. [PubMed: 12297761]

44. Huang D, Swanson EA, Lin CP, Schuman JS, Stinson WG, Chang W, Hee MR, Flotte T, Gregory K, Puliafito CA, et al. Optical coherence tomography. Science 1991;254:1178–1181. [PubMed: 1957169]
45. Tearney GJ, Brezinski ME, Bouma BE, Boppart SA, Pitris C, Southern JF, Fujimoto JG. In vivo endoscopic optical biopsy with optical coherence tomography. Science 1997;276:2037–2039. [PubMed: 9197265]
46. Rollins AM, Ung-Runyawee R, Chak A, Wong CK, Kobayashi K, Sivak MV, Izatt JA. Real-time in vivo imaging of human gastrointestinal ultrastructure by use of endoscopic optical coherence tomography with a novel efficient interferometer design. Optics Lett 1999;24:1358–1360.
47. Kobayashi K, Izatt JA, Kulkarni MD, Willis J, Sivak MV Jr. High-resolution cross-sectional imaging of the gastrointestinal tract using optical coherence tomography: preliminary results. Gastrointest Endosc 1998;47:515–523. [PubMed: 9647378]
48. Sivak MV Jr, Kobayashi K, Izatt JA, Rollins AM, Ung-Runyawee R, Chak A, Wong RC, Isenberg GA, Willis J. High-resolution endoscopic imaging of the GI tract using optical coherence tomography. Gastrointest Endosc 2000;51:474–479. [PubMed: 10744825]
49. Drexler W, Morgner U, Ghanta RK, Kartner FX, Schuman JS, Fujimoto JG. Ultrahigh-resolution ophthalmic optical coherence tomography. Nat Med 2001;7:502–507. [PubMed: 11283681]
50. Poneros JM, Brand S, Bouma BE, Tearney GJ, Compton CC, Nishioka NS. Diagnosis of specialized intestinal metaplasia by optical coherence tomography. Gastroenterology 2001;120:7–12. [PubMed: 11208708]
51. Bouma BE, Tearney GJ, Compton CC, Nishioka NS. High resolution of the human esophagus and stomach in vivo using optical coherence tomography. Gastrointest Endosc 2000;51:467–474. [PubMed: 10744824]
52. Pfau PR, Sivak MV Jr, Chak A, Kinnard M, Wong RC, Isenberg GA, Izatt JA, Rollins A, Westphal V. Criteria for the diagnosis of dysplasia by endoscopic optical coherence tomography. Gastrointest Endosc 2003;58:196–202. [PubMed: 12872085]
53. Pawley, J., editor. Handbook of biological confocal microscopy. 3. New York: Plenum; 1996.
54. Sabharwal YS, Rouse AR, Donaldson L, Hopkins MF, Gmitro AF. Slit-scanning confocal microendoscope for high-resolution in vivo imaging. Appl Optics 1999;38:7133–7144.
55. Liang C, Sung K, Richards-Kortum R, Descour MR. Design of a high-numerical-aperture miniature microscope objective for an endoscopic fiber confocal reflectance microscope. Appl Optics 2002;41:4603–4610.
56. Delaney PM, Harris MR, King RG. Fiber-optic laser scanning confocal microscope suitable for fluorescence imaging. Applied Optics 94;33:573–577.
57. Kiesslich R, Burg J, Vieth M, Gnaendiger J, Enders M, Delaney P, Polglase A, McLaren W, Janell D, Thomas S, Nafe B, Galle PR, Neurath MF. Confocal laser endoscopy for diagnosing intraepithelial neoplasias and colorectal cancer in vivo. Gastroenterology 2004;127:706–713. [PubMed: 15362025]
58. Wang TD, Contag CH, Mandella MJ, Kino GS. Dual axes confocal microscope with post-objective scanning and low coherence heterodyne detection. Optics Lett 2003;28:1915–1917.
59. Wang TD, Contag CH, Mandella MJ, Chan NY, Kino GS. Confocal fluorescence microscope with dual axis architecture and biaxial postobjective scanning. J Biomed Opt 2004;9:735–742. [PubMed: 15250760]
60. Dickensheets DL, Kino GS. A micromachined scanning confocal optical microscope. Optics Lett 1996;21:764–766.
61. Backman V, Wallace MB, Perelman LT, Arendt JT, Gurjar R, Muller MG, Zhang Q, Zonios G, Kline E, McGilligan JA, Shapshay S, Valdez T, Badizadegan K, Crawford JM, Fitzmaurice M, Kabani S, Levin HS, Seiler M, Dasari RR, Itzkan I, Van Dam J, Feld MS, McGillican T. Detection of preinvasive cancer cells. Nature 2000;406:35–36. [PubMed: 10894529]
62. Georgakoudi I, Jacobson BC, Van Dam J, Backman V, Wallace MB, Muller MG, Zhang Q, Badizadegan K, Sun D, Thomas GA, Perelman LT, Feld MS. Fluorescence, reflectance, and light-scattering spectroscopy for evaluating dysplasia in patients with Barrett's esophagus. Gastroenterology 2001;120:1620–1629. [PubMed: 11375944]

63. Wallace MB, Perelman LT, Backman V, Crawford JM, Fitzmaurice M, Seiler M, Badizadegan K, Shields SJ, Itzkan I, Dasari RR, Van Dam J, Feld MS. Endoscopic detection of dysplasia in patients with Barrett's esophagus using light-scattering spectroscopy. Gastroenterology 2000;119:677–682. [PubMed: 10982761]

64. Roy HK, Liu Y, Wali RK, Kim YL, Kromine AK, Goldberg MJ, Backman V. Four-dimensional elastic light-scattering fingerprints as preneoplastic markers in the rat model of colon carcinogenesis. Gastroenterology 2004;126:1071–1081. [PubMed: 15057746]

65. Bakker Schut TC, Witjes MJ, Sterenborg HJ, Speelman OC, Roodenburg JL, Marple ET, Bruining HA, Puppels GJ. In vivo detection of dysplastic tissue by Raman spectroscopy. Anal Chem 2000;72:6010–6018. [PubMed: 11140770]

66. Kendall C, Stone N, Shepherd N, Geboes K, Warren B, Bennett R, Barr H. Raman spectroscopy, a potential tool for the objective identification and classification of neoplasia in Barrett's oesophagus. J Pathol 2003;200:602–609. [PubMed: 12898596]

67. Shim MG, Song LM, Marcon NE, Wilson BC. In vivo near-infrared Raman spectroscopy: demonstration of feasibility during clinical gastrointestinal endoscopy. Photochem Photobiol 2000;72:146–150. [PubMed: 10911740]

68. Molckovsky A, Song LM, Shim MG, Marcon NE, Wilson BC. Diagnostic potential of near-infrared Raman spectroscopy in the colon: differentiating adenomatous from hyperplastic polyps. Gastrointest Endosc 2003;57:396–402. [PubMed: 12612529]

69. Massoud TF, Gambhir SS. Molecular imaging in living subjects: seeing fundamental biological processes in a new light. Genes Dev 2003;17:545–580. [PubMed: 12629038]

70. Mahmood U, Weissleder R. Near-infrared optical imaging of proteases in cancer. Mol Cancer Ther 2003;2:489–496. [PubMed: 12748311]

71. Marten K, Bremer C, Khazaie K, Sameni M, Sloane B, Tung C, Weissleder R. Detection of dysplastic intestinal adenomas using enzyme-sensing molecular beacons in mice. Gastroenterology 2002;122:406–414. [PubMed: 11832455]

72. Funovics MA, Alencar H, Su HS, Khazaie K, Weissleder R, Mahmood U. Miniaturized multichannel near infrared endoscope for mouse imaging. Mol Imaging 2003;2:350–357. [PubMed: 14717334]

Abbreviations used in this paper

ALA
aminolevulinic acid

APC
adenomatous polyposis coli

CCD
charge coupled device

HGD
high-grade dysplasia

LGD
low-grade dysplasia

LSS
light-scattering spectroscopy

NIR
near-infrared

OCT
optical coherence tomography

PPIX

protoporphyrin IX

UV

ultraviolet

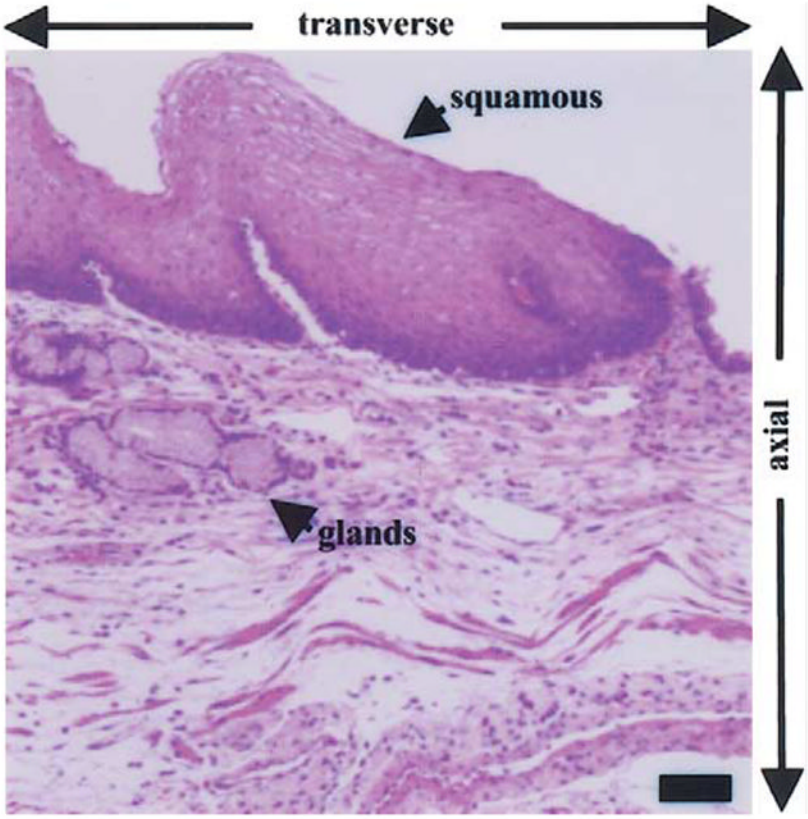

Figure 1.
Histological examination of esophagus shows the presence of glands below the squamous epithelium, illustrating the need for optical methods to evaluate below the mucosal surface and for sub-cellular resolution in the axial and transverse dimensions. Scale bar, 50 μm. (Hematoxylin and eosin.)

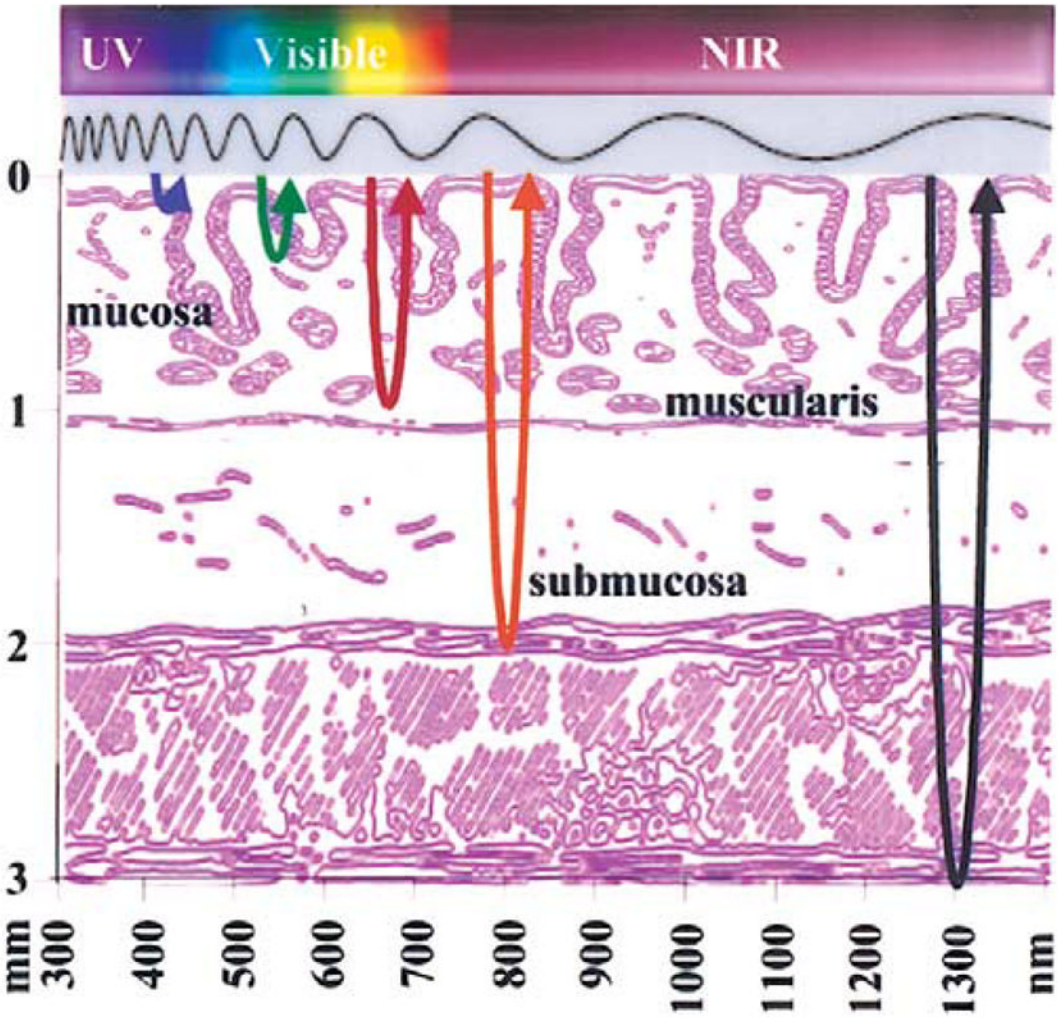

Figure 2.
Electromagnetic spectrum used for novel methods of optical biopsy includes ultraviolet (UV), visible, and near-infrared (NIR) light, resulting in different depths of tissue penetration through the mucosa (graded layers) and submucosa (>1 mm depth).

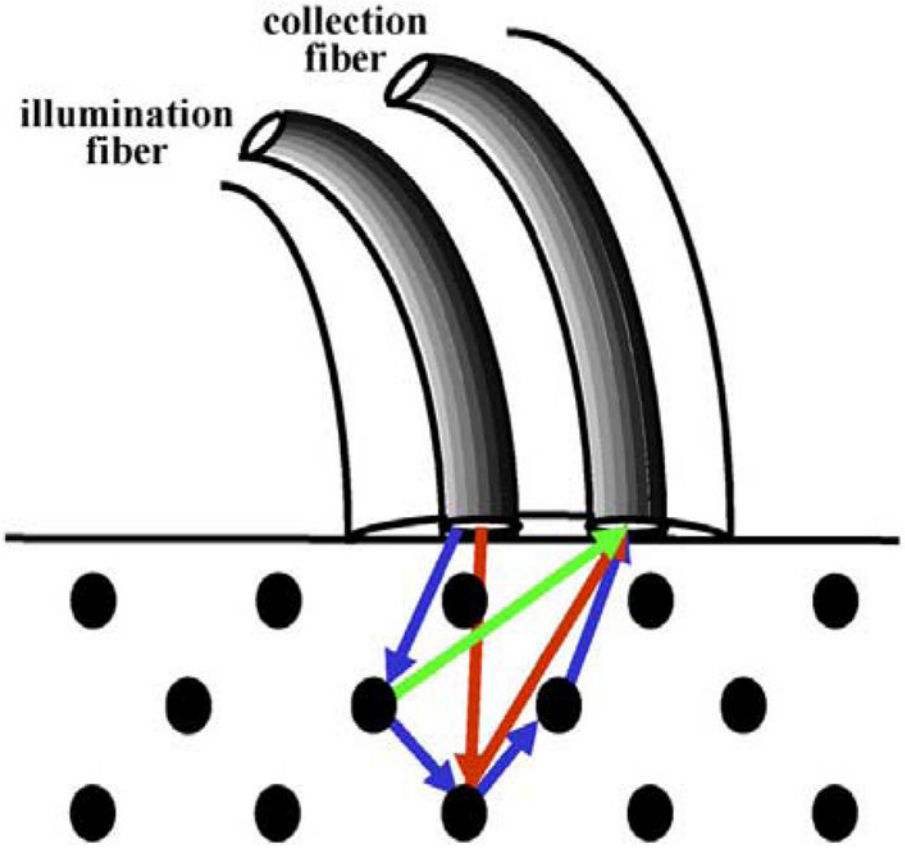

Figure 3.
Optical fiber probes can be used for mucosal point detection to collect elastic (*red arrows*) or inelastic (*green arrow*) scattered light. Ballistic (*red arrows*) and diffuse (*blue arrows*) photons return after a single and several scattering events, respectively.

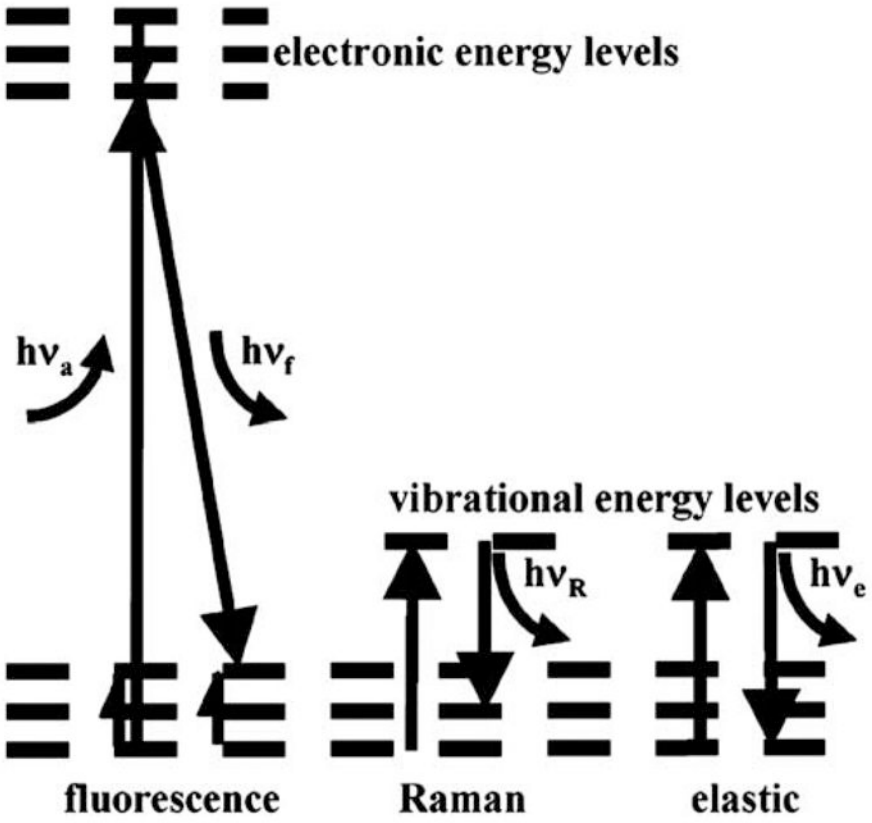

Figure 4.

Light absorbed by biomolecules ($h\nu_a$) is released as transitions occur between energy levels. Fluorescence ($h\nu_f$) results from electrons relaxing to the ground state, releasing light at wavelengths longer than that of incident. Raman (inelastic) and elastic scattering occur when biochemical functional groups change in vibrational energy levels.

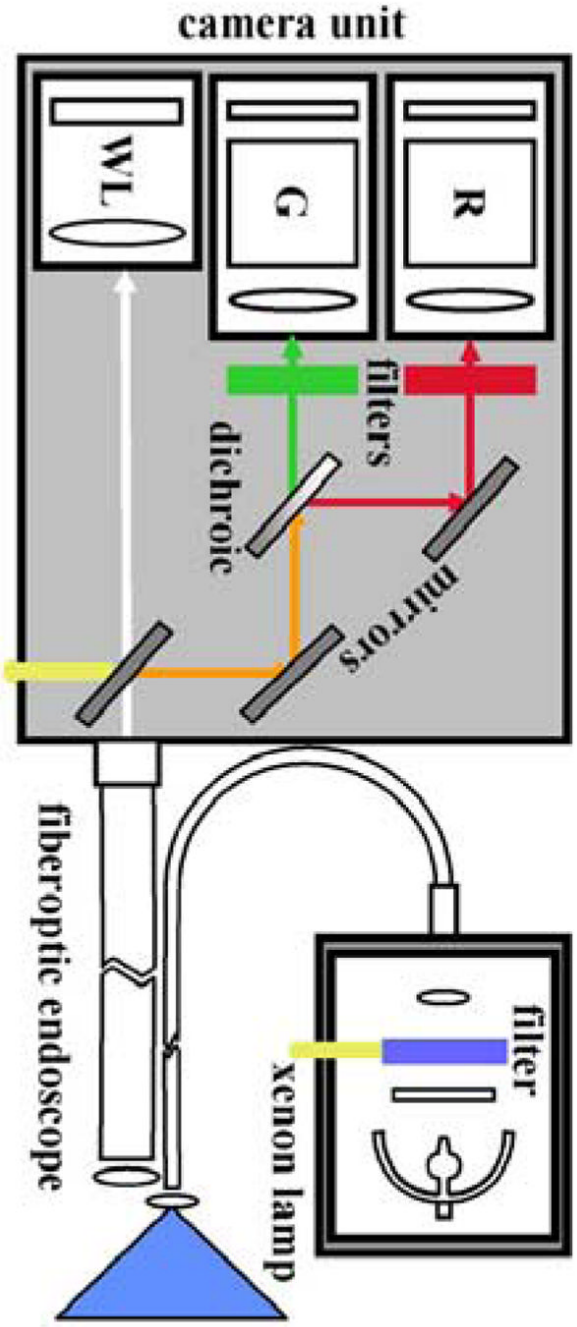

Figure 5.
Schematic of LIFE camera unit. Excitation provided by blue light from a filtered xenon lamp produces fluorescence that is collected by a fiber-optic endoscope. The red (R) and green (G) spectral components are separated by a dichroic, bandpass filtered, and then imaged by two separate intensified cameras. A mirror can be flipped away to allow detection of white light (WL).

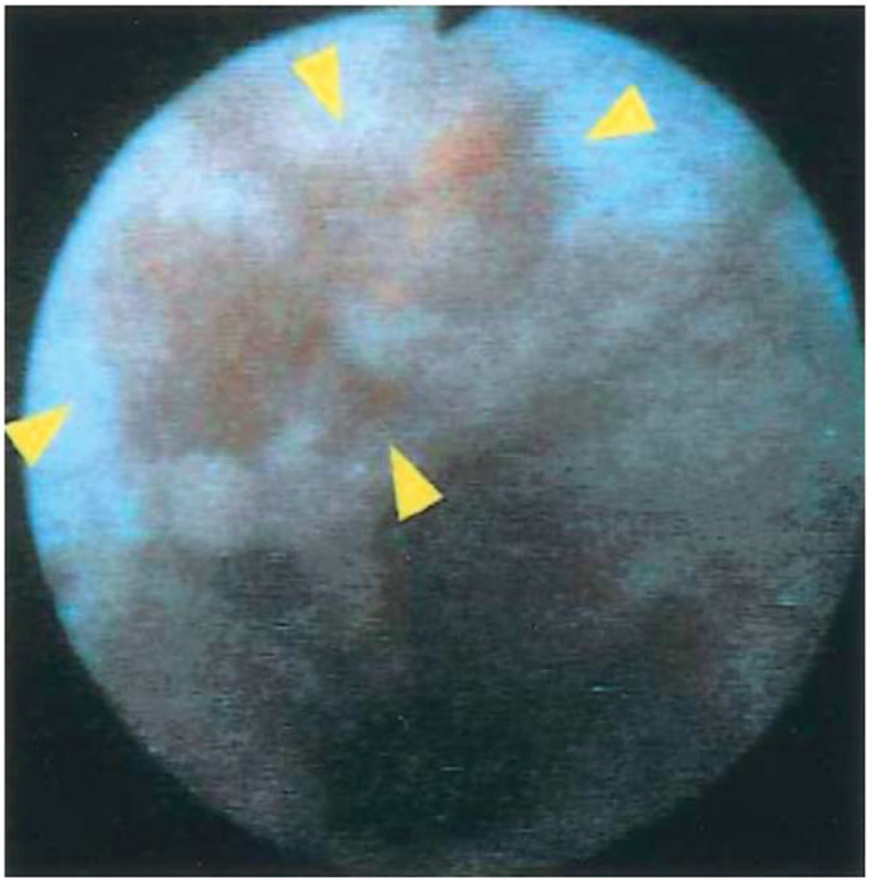

Figure 6.
Focus of high-grade dysplasia (*arrowheads*) localized within Barrett's segment revealed by fluorescence collected with LIFE endoscopy system. Reprinted with permission.[35]

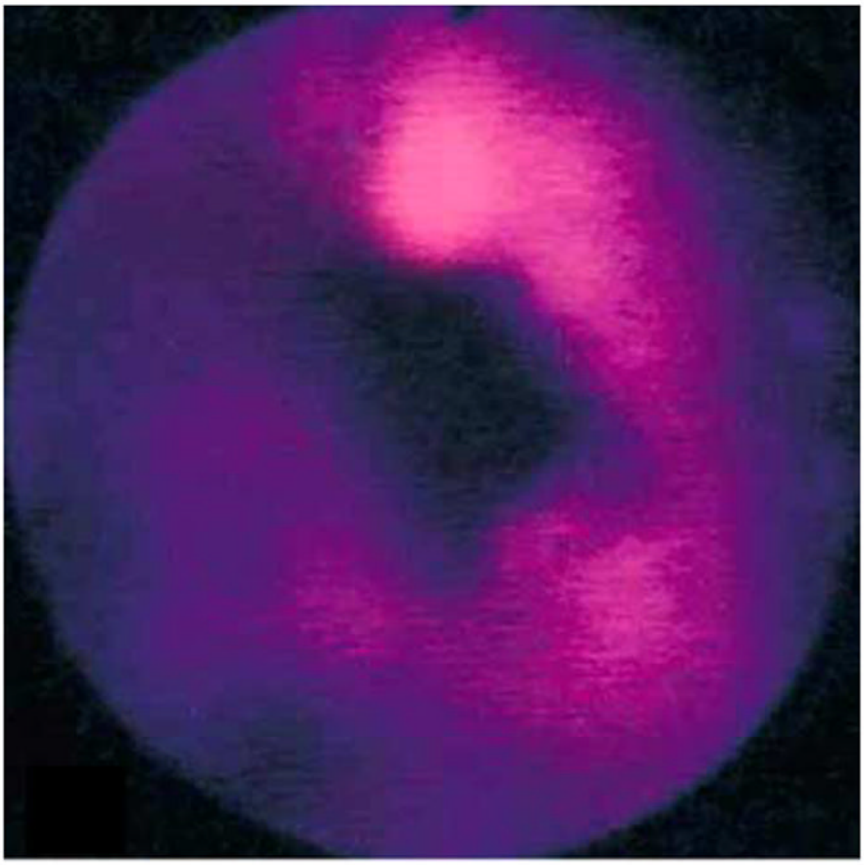

Figure 7.
Red fluorescence image of aminolevulinic acid–induced protoporphyrin IX from distal esophagus shows a superficial esophageal carcinoma that was not visible on white light. Reprinted with permission.[42]

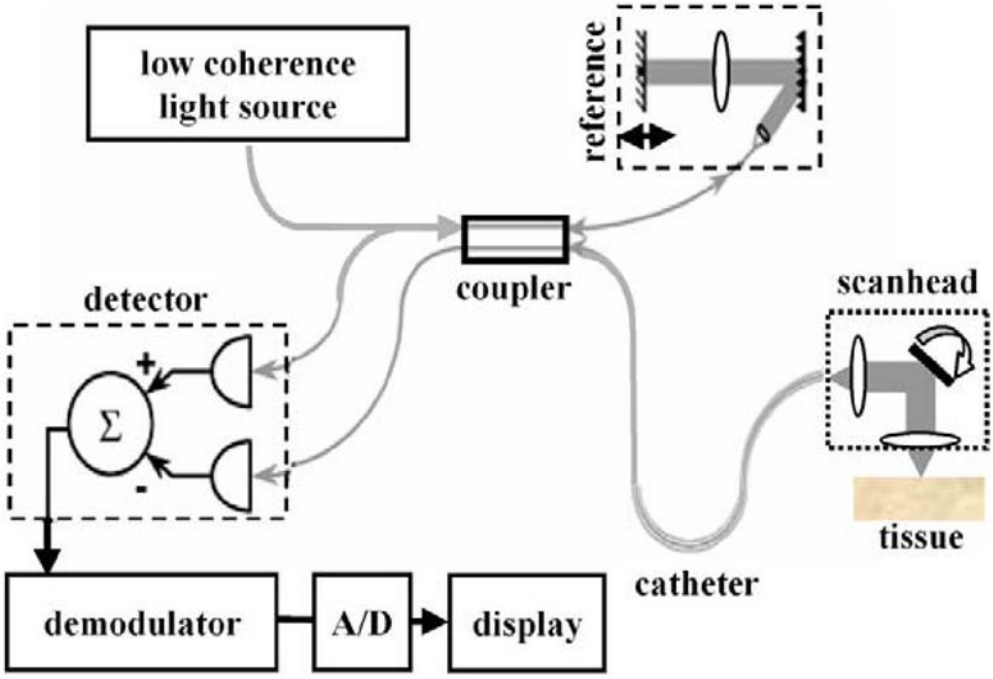

Figure 8.
Schematic of optical circuit in optical coherence tomography imaging system.

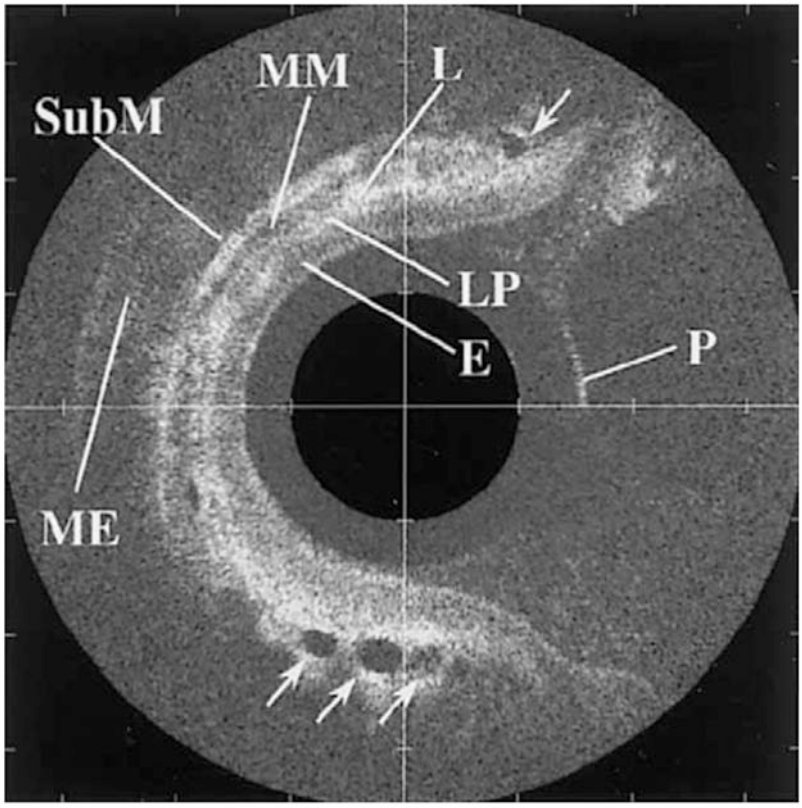

Figure 9.
Optical coherence tomographic image from normal esophagus shows outer surface of the probe (P) and discrete layers of mucosa, including squamous epithelium (E), lamina propria (LP), muscularis mucosa (MM), submucosa (SubM), lymph nodes (L), and muscularis externa (ME). Reprinted with permission.[46]

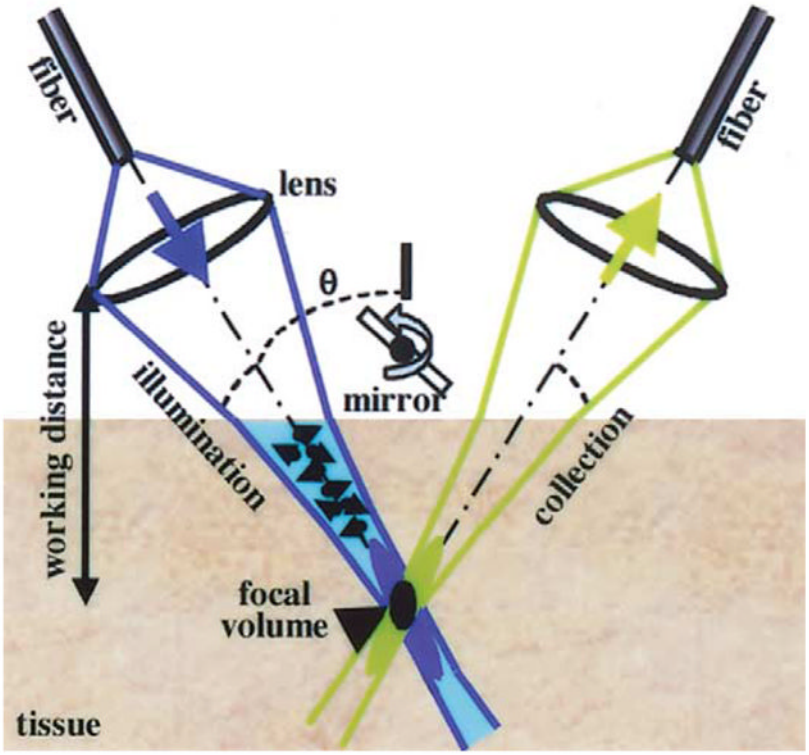

Figure 10.
Dual-axes confocal architecture uses separate illumination and collection objectives to reduce axial resolution (*black oval*), increase long working distance, and decrease light scattering.

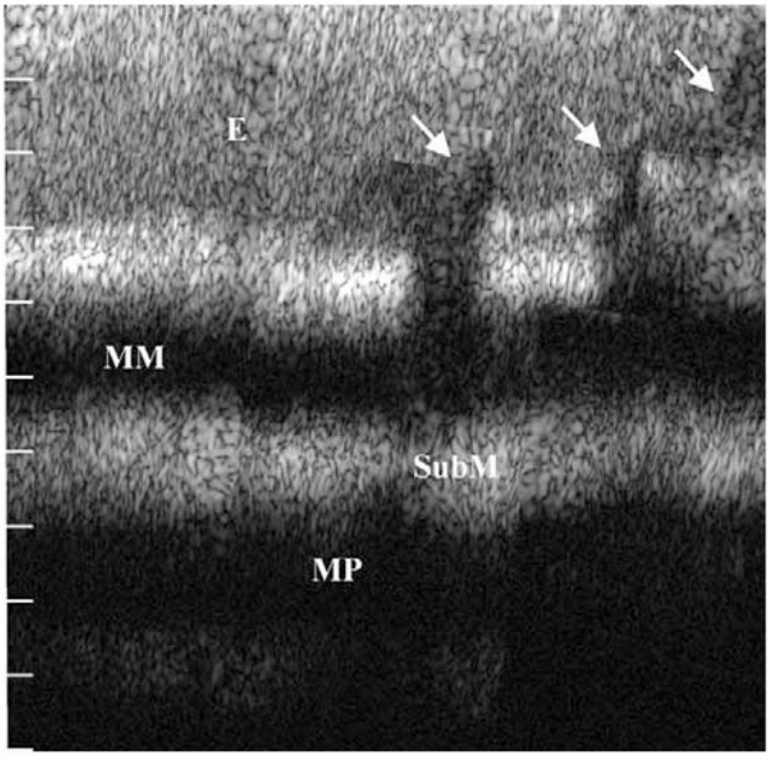

Figure 11.
Dual-axes confocal image of the neosquamocolumnar metaplastic junction of resected human esophagus shown over a depth of 1 mm shows intact squamous epithelium (E), muscularis mucosa (MM), submucosa (SubM), and muscularis propria (MP) on the left and columnar mucosa with pit epithelium (*arrows*) on the right. Reprinted with permission.[58]

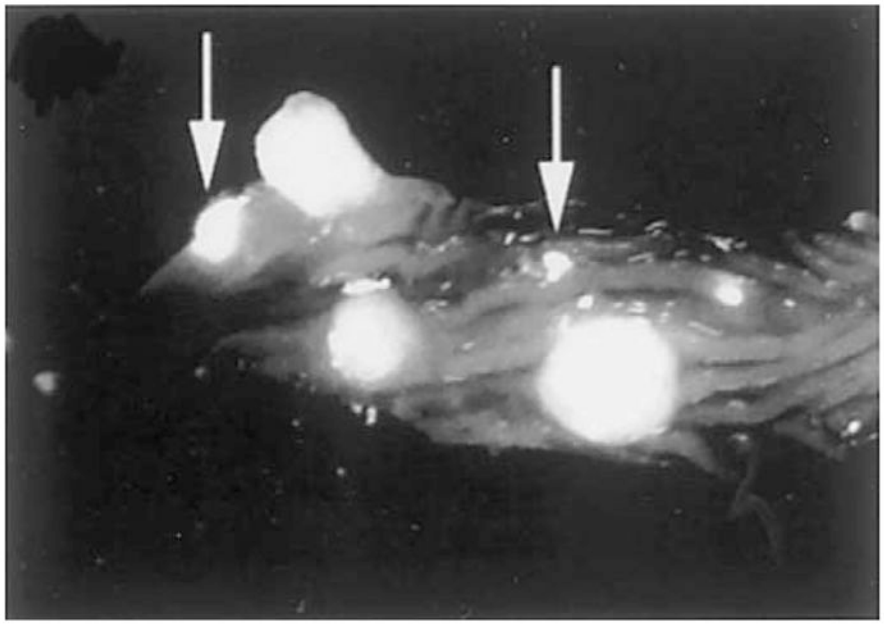

Figure 12.
Near-infrared fluorescence image of an excised specimen of the colon from an APC min mouse after injection with the cathepsin B probe. Several 2–5-mm diameter polyps and adenomas as small as 50 μm (*arrows*) can be seen. Reprinted with permission.[71]

Table 1

Clinical End Points for Optical Biopsy in the Gastrointestinal Tract

Minimize number of target biopsies and frequency of surveillance
Detect and localize high-grade dysplasia in Barrett's esophagus
Identify neoplasia beneath neosquamous esophageal mucosa
Assess depth of tumor invasion for possible mucosal resection
Preoperative identification of tumor margins
Evaluate effectiveness of pharmacological therapy
Detect and localize dysplasia in the setting of ulcerative colitis
Distinguish adenomatous from hyperplastic polyps
Avoid biopsy in patients with bleeding diatheses
Surveillance of polypectomy and mucosal resection site
Differentiate malignant and benign ulcers and strictures

Table 2

Summary of Light-Tissue Interaction Mechanisms and Potential Clinical Use

Method	Light-tissue interaction mechanism	Potential clinical use
Fluorescence endoscopy	Endogenous biomolecules, photosensitizers	Wide-area surveillance
Optical coherence tomography	Backscatter, low-coherence interferometry	Cross-sectional histopathologic examination
Confocal microscopy	Backscatter, spatial filtering	Cross-sectional histopathologic examination
Light-scattering spectroscopy	Elastic scattering, diffuse visible photons	Subcellular morphological examination
Raman spectroscopy	Inelastic scattering, diffuse near-infrared photons	Molecular histopathologic examination
Molecular imaging	Fluorescence triggered by molecular interaction	Molecular imaging

Table 3

Comparison of Performance of Optical Biopsy Methods

Method	FOV	Penetration depth (μm)	Axial resolution	Transaxial resolution	Contrast
Fluorescence endoscopy	4^+	<100	1^+	1^+	$3–4^+$
Optical coherence tomography	$1–2^+$	>1000	$3–4^+$	$3–4^+$	$1–2^+$
Confocal microscopy	$1–2^+$	>1000	4^+	4^+	$1–4^+$
Light-scattering spectroscopy	1^+	<1000	—	—	—
Raman spectroscopy	1^+	>1000	—	—	—
Molecular beacons	4^+	>1000	1^+	1^+	4^+

Table 4

Glossary of Technical Terms

Term	Description
Ballistic photons	Light detected after undergoing single backscattering event
Charge-coupled device	Silicon image detector sensitive to both visible and near-infrared light
Coherence	Spatial extent over which light has reliable phase
Confocal	Reduction of scattering by spatially limiting light beam with pinholes
Diffuse scattering	Photons that undergo multiple backscattering events
Elastic scattering	Photons backscattered with same wavelength as that of incident
Field of view	Surface area of mucosa imaged by detector
Fluorescence	Light emitted by electrons relaxing from higher to lower energy levels
Inelastic scattering	Photons backscattered with a longer wavelength than that of incident
Mie theory	Mathematical description of light scattering by particles of all sizes
Molecular beacons	Probe that releases fluorescence after specific molecular interaction
Optical biopsy	Nondestructive in situ assay of tissue histopathologic characteristics using light
Micro-electro-mechanical systems	Microfabrication of silicon substrate suitable for mass production
Near-infrared	Light with wavelengths longer than that of red, not visible to human eye
Numerical aperture	Angle of light convergence within tissue produced by objective
Raman scattering	Inelastic scattering by vibrational/rotational modes of molecular bonds
Working distance	Distance between region of focus and closest surface of objective